A putative type V pilus contributes to *Bacteroides thetaiotaomicron* biofilm formation capacity

Jovana MIHAJLOVIC[1,2,7]; Nathalie BECHON[1,2];Christa IVANOVA[1]; Florian CHAIN[3]; Alexandre ALMEIDA[4,5,6,8]; Nathalie BECHON[1,2], Philippe LANGELLA[3]; Christophe BELOIN[1]; and Jean-Marc GHIGO[1]

[1] *Institut Pasteur, Genetics of Biofilms Laboratory. 25-28 rue du Docteur Roux, 75015 Paris,cedex 15, France.*

[2] *Universite Paris Diderot, Bio Sorbonne Paris Cite (BioSPC), Paris cedex, France.*

[3]*Commensals and Probiotics-Host Interactions Laboratory, Micalis Institute, INRA, AgroParisTech, Université Paris-Saclay, 78350, Jouy-en-Josas, France.*

[4]*Institut Pasteur, Unité Evolution et Ecologie de la Résistance aux Antibiotiques, Paris, France.*

[5]*CNRS UMR 3525, Paris, France.*

[6]*Université Pierre et Marie Curie, Paris, France.*

[7] *Present address: Department of Microbiology and Ecosystem Science, Division of Microbial Ecology, Research Network Chemistry Meets Microbiology, University of Vienna, Althanstrasse 14, Vienna, Austria.*

[8]*Present address: EMBL-EBI European Bioinformatics Institute, Wellcome Genome Campus, Hinxton, Cambridge CB10 1SD, UK.*

Corresponding author:

Jean-Marc Ghigo (jmghigo@pasteur.fr)

Running Title: *Bacteroides thetaiotaomicron* biofilm formation

ABSTRACT

Bacteroides thetaiotaomicron is a prominent anaerobe member of the healthy human gut microbiota. While the majority of functional studies on *B. thetaiotaomicron* addressed its impact on the immune system and the utilization of diet polysaccharide, *B. thetaiotaomicron* biofilm capacity and its contribution to intestinal colonization are still poorly characterized. We tested the natural adhesion of 34 *B. thetaiotaomicron* isolates and showed that, although biofilm capacity is widespread among *B. thetaiotaomicron* strains, this phenotype is masked or repressed in the widely used reference strain VPI 5482. Using transposon mutagenesis followed by a biofilm positive selection procedure we identified VPI 5482 mutants with increased biofilm capacity corresponding to an alteration in the C-terminal region of BT3147, encoded by the *BT3148-BT3147* locus, which displays homology with mfa-like typeV pili found in many *Bacteroidetes*. We showed that BT3147 is exposed on *B. thetaiotaomicron* surface and that BT3147-dependent adhesion also requires BT3148, suggesting that BT3148-BT3147 correspond to the anchor and stalk subunits of a new type V pilus involved in *B. thetaiotaomicron* adhesion. This study therefore introduces *B. thetaiotaomicron* as a model to study proteinaceous adhesins and biofilm-related phenotypes in this important intestinal symbiont.

IMPORTANCE

Although the gut anaerobe *Bacteroides thetaiotaomicron* is a prominent member of the healthy human gut microbiota, little is known on its capacity adhere to surfaces and form biofilms. Here, we identified that alteration of a surface exposed protein corresponding to a type of pili found in many *Bacteroidetes* increases *B. thetaiotaomicron* biofilm formation. This study lays the ground for establishing this bacterium as a model organism for *in vitro* and *in vivo* study of biofilm-related phenotypes in gut anaerobes.

KEYWORDS

Biofilm; *Bacteroides thetaiotaomicron*; gut commensal, adhesion, typeV pili

INTRODUCTION

Bacterial biofilms are widespread surface-attached communities, in which reduced diffusion and a heterogeneous structure favor physical and metabolic contacts between bacteria and induce novel behaviors as compared to individual planktonic microorganisms (1, 2). In the past decades, biofilms were often investigated under aerobic conditions using genetically amenable aerobic bacterial models, and anaerobic biofilms studies mainly focused on oral anaerobes. Although these studies considerably advanced our understanding of this important bacterial lifestyle, many clinically and ecologically important processes take place in anaerobic conditions and are carried out by strict or facultative commensal and pathogenic anaerobes (3). This is in particular the case of the vertebrate gut microbiota, which is vastly dominated by anaerobic Firmicutes and Bacteroidetes (4, 5). However, although the intestinal microbiota provides protection from pathogen colonization and impacts host intestinal physiology and health (6-11), the contributions of its structural organization and of the biofilm-formation capacities of gut anaerobes are still poorly understood.

One of the most abundant and best-studied members of the healthy human gut microbiota is the strictly anaerobic bacterium *Bacteroides thetaiotaomicron* (12). *B. thetaiotaomicron* was shown to contribute to the development of the intestinal mucosal layer, modulate the function of the intestinal immune system and is considered to play a key role in the breakdown of diet and host-derived polysaccharides (13-16). Whereas biofilm formation could be involved in several important aspects of *B. thetaiotaomicron* biology, including intestinal colonization, inter- and intra-species interactions and virulence in extra-intestinal sites (17, 18), studies investigating *B. thetaiotaomicron* adhesion and biofilm formation are still scarce. A transcriptomic analysis performed on biofilm formed on carbon paper surface in chemostats showed an upregulation of several polysaccharide utilization loci (PUL) involved in polysaccharide foraging, mucin degradation enzymes, as well as of two out of eight *B. thetaiotaomicron* capsular systems (19). This study, however, did not reveal significant differences in the expression level of genes encoding extracellular appendages usually associated with bacterial surface-adhesion, leaving open the question whether adhesins contribute to *B. thetaiotaomicron* biofilm formation.

In the present study, we showed that, although *in vitro* biofilm development is widespread among natural *B. thetaiotaomicron* isolates, the reference *B. thetaiotaomicron* VPI 5482

(ATCC 29148) commonly used in human gut microbiota studies forms poor biofilm. We hypothesized that functions involved in VPI 5482 *in vitro* biofilm formation could be repressed or masked and use of transposon mutagenesis and a positive selection procedure allowed us to identify a mutation in the gene *BT3147*, altering the C-terminal region of BT3147 and increasing VPI 5482 biofilm formation. We showed that the *BT3148-BT3147* locus displays homology with the Mfa-like type V pili found in many *Bacteroides* species (20) and could encode a surface exposed type V pilus involved in *B. thetaiotaomicron* adhesion. We expect this work to lay the ground for further characterization of B. thetaiotaomicron adhesins in VPI5482 and other biofilm-forming isolates, establishing this species as a model organism for in vitro and in vivo study of biofilm-related phenotypes in gut anaerobes

RESULTS

The reference strain *B. thetaiotaomicron* VPI 5482 forms poor *in vitro* biofilm

In order to analyze the ability of *B. thetaiotaomicron* VPI 5482 (ATCC 29148) (12) to form biofilm, we performed *in vitro* biofilm assays, using either a static 96-well plate model followed by crystal violet staining or dynamic continuous-flow biofilm microfermenters. Although *B. thetaiotaomicron* VPI 5482 adhesion and biofilm formation was previously reported in chemostat on carbon paper (19), we observed poor or no biofilm formation in both biofilm models (Fig. 1A and 1C). We then tested the biofilm capacity of 34 *B. thetaiotaomicron* isolates (Table S1) and found that 41% of them (14 out of 34) produce more biofilm than VPI 5482 (Fig. 1AB and Fig. S1). Taken together, these results indicate that, whereas the ability to form biofilm is widespread among natural *B. thetaiotaomicron* isolates, the widely used reference strain VPI5482 is a poor biofilm former in the tested growth conditions.

Selection of *B. thetaiotaomicron* VPI 5482 mutants with increased biofilm capacity

Considering the ability of several *B. thetaiotaomicron* strains to form biofilm, we hypothesized that functions involved in biofilm formation could be repressed or masked in the *B. thetaiotaomicron* VPI 5482 strain. To test this hypothesis and identify *B. thetaiotaomicron* VPI 5482 mutants with increased biofilm formation ability, we generated a library of over 10,000 mariner transposon mutants and subjected them to a positive selection procedure for biofilm formation. Briefly, we resuspended a mix of *B. thetaiotaomicron* VPI 5482 transposon mutants in a tube with 15 ml of BHIS medium (adjusted to OD_{600}=1) and we placed a microfermenter glass spatula into this solution for 10 minutes, to allow for initial adhesion (Fig. 2A). The spatula was then washed in BHIS medium to remove non-adherent bacteria. Subsequently, the spatula potentially carrying the most adherent mutants was inserted in a continuous-flow biofilm microfermenter to allow surface growth and favor positive selection of *B. thetaiotaomicron* mutants with increased adhesion capacity. After 8 hours the spatula-associated bacterial population was re-suspended in fresh BHIS medium and the resulting overnight culture was used as the inoculum for another cycle of positive selection (Fig. 2A). After 4 cycles of positive selection, the biofilm microfermenter inoculated with culture potentially enriched in biofilm positive *B. thetaiotaomicron* VPI 5482 mutants displayed, after 24h, a strong biofilm formation compared to a microfermenter inoculated with the original wild type VPI 5482 strain (Fig. 2B). After resuspension of the corresponding

biofilm, *B. thetaiotaomicron* VPI 5482 mutants were subjected to serial dilution in BHIS and plated on selective agar plates. We re-isolated the resulting colonies and individually tested mutants using 96-well plate biofilm assay. This led us to identify several mutants with an improved biofilm–forming capacity compared to WT VPI 5482.

Transposon insertion in the 3'end of the Mfa/type V pilin homolog gene *BT3147* increases biofilm formation

We determined that 8 of the identified biofilm positive mutants (Fig. 2C), had a transposon inserted in *BT3147,* a gene located downstream of *BT3148* and upstream of *BT3146-BT3145* (Fig. 3A). Although protein sequence analysis only showed weak homologies, search in structure databases revealed that the N-terminal region (Residues 49 to 192) and the central region of BT3147 (residues 171 to 388) contain a pfam 08842 (Mfa2) domain corresponding to Mfa2/Mfa1 pilin of recently defined type V pili that are ubiquitous in *Porphyromonas gingivalis* and other gut Bacteroidetes (20). All eight transposon insertions were located in the last 40 codons of *BT3147* and produced three different deletion/insertion events in *BT3147* coding sequence (Figure 3B). Class 1 mutants (3 mutants 2D7; 2D12; 2B9; see Figure 2C) correspond to an out of frame transposon insertion at position 1138 bp, deleting the last 9 amino acids from *BT3147* without adding any transposon-derived coding sequence (hereafter named *BT3147*Δ*9*). One representative of class 1, 2D7, was chosen for further analysis. Class 2 mutants (3 mutants 1A8; 1H2; 2A12; see Figure 2C) correspond to an in-frame transposon insertion at position 1047, deleting the last 40 amino acids of BT3147 and replacing them by 50 amino acids from the transposon sequence leading to a chimeric 398 codon sequence (*BT3147*Δ*40+50*). One representative of class 2, 1H2, was chosen for further analysis. Finally, Class 3 mutants (2 mutants 1H9, 3F12; see Figure 2C) correspond to a 434 amino acid fusion protein arising from the deletion of the last 3 *BT3147* codons replaced by 49 codons from the transposon sequence (*BT3147*Δ*3+49*) (Fig. 3B).

To confirm the link between biofilm production and transposon insertion in *BT3147,* we deleted gene *BT3147* in the wild type VPI 5482 strain, however this approach did not lead to an increase in biofilm formation (Fig. 3C). We then hypothesized that insertion of the transposon in the 3' extremity of *BT3147* could prevent (by polar effect) or enhance the expression of the downstream genes *BT3146* and *BT3145* (Fig. 3A). However, deletion of *BT3146-BT3145* did not lead to significant alteration of biofilm formation compared to WT VPI 5482 strain (Fig. 3C). In addition, the comparison of VPI 5482 and 1H2 transcription using RNAseq analysis showed that the insertion of the transposon did not alleviate a

potential premature transcription termination in the wild type strain. Moreover, we did not detect any antisense transcript in the *BT3147-5* region that could be interfering with *BT3147* transcription (Fig. S2). Nevertheless, deletion of the 1046 base pairs of *BT3147* (1167 bp) located upstream of the transposon insertion point in the class2 1H2 mutant, the strongest biofilm former among our 8 mutants (Figure 2C), abolished biofilm formation in this strain (Fig. 3D). This result demonstrated that the presence of the mariner transposon *per se* does not promote biofilm formation and that the observed biofilm phenotype requires at least part of the *BT3147* gene.

C-terminal truncation of BT3147 promotes BT3148-dependent *B. thetaiotaomicron* biofilm formation

We then further investigated the consequences of transposon insertions on the BT3147 protein by reproducing one of the genetic configurations created by transposon insertion. We chose class 1 biofilm-forming mutants, as they correspond to the truncation of BT3147 nine last C-terminal amino-acids (*BT3147*Δ*9)* without added transposon-derived coding sequence. Since downstream genes *BT3146* and *BT3145* are not involved in the studied phenotype (Fig. 3C, Fig. S2), we constructed a chromosomal *BT3147*Δ*9 de novo* by removing the VPI 5482 region encompassing the last 9 codons of *BT3147* and the downstream genes *BT3146* and *BT3145*, replacing it by a stop codon (Fig. 4A). We then compared the resulting strain, *BT3147Δ9* Δ*BT3146-45* with the wild type strain VPI 5482 and showed that it displayed an increased biofilm formation capacity (Fig. 4A and supplementary Fig.S3). Consistently, whereas chromosomal-based expression of *BT3148-BT3147* displayed a wild type biofilm phenotype, expression of *BT3148-BT3147*Δ*9* led to increased biofilm formation compared to WT VPI 5482 (Fig. 4A).

Use of an antiserum raised against BT3147 enabled the immunodetection of a truncated form of BT3147 in whole cell extracts of strain *BT3147*Δ*9* Δ*BT3146-45*, class 1 (2D7), class 2 (1H2) transposon mutants and in the wild type strain constitutively expressing *BT3147*Δ*9* (Fig. 4B). However, while WT (40.6 kDa) and truncated versions of BT3147 (1H2, 41.6 kDa; 2D7 and *de novo* BT3147Δ9, 39.6 kDa) have very similar theoretical size, the truncated forms of BT3147 migrated at an apparent smaller molecular mass of ~30-35kDa, suggesting an additional cleavage of these forms (see discussion).

Finally, considering that BT3148, encoded by the gene located immediately upstream of *BT3147* (Figure 3A*)* displays homology with the *B. thetaiotaomicron* Fim2B/Mfa2 homolog BT2657 (PDB code c3gf8A), we tested BT3148 contribution to BT3147Δ9-dependent biofilm

formation. Deletion of *BT3148* in *B. thetaiotaomicron BT3147Δ9* Δ*BT3146-45* resulted in a significant decrease in biofilm formation (Fig. 4C). Taken together, these results demonstrated that a C-terminal truncation of BT3147 promote biofilm formation in *B. thetaiotaomicron*.

Localization of a putative BT3148-BT3147 type V pilus on *B. thetaiotaomicron* surface

BT3148 and BT3147 display structural similarities with Mfa1/ type V pili identified in the anaerobic oral pathogen *P. gingivalis* and other gut Bacteroidetes (20). Two types of pili were described in *P. gingivalis* – the long FimA and the short Mfa1. FimA filaments are more than 1 μm long, fragile and promote autoaggregation and biofilm formation (21). FimA corresponds to the major structural component of the FimA filaments, FimB to the anchor protein, and FimC-E to accessory proteins (22). The shorter Mfa1 type pili are 0.1 – 0.5 μm long filaments essentially composed of the major stalk protein Mfa1, bound to the cell surface via the membrane-located anchor protein Mfa2 (Fig. 5 A). In addition to *mfa1* and *mfa2*, the *P. gingivalis* gene cluster often includes genes *mfa3-5*, which encode accessory proteins. Since BT3148 displays homology with *B. thetaiotaomicron* Fim2B/Mfa2 homolog BT2657 (PDB code c3gf8A), we propose that it could be a *B. thetaiotaomicron* VPI 5482 type V pilus anchor (Fig. 5 A and Fig. S3). BT3147, on the other hand displays structural homology with *Bacteroides eggerthii* DSM 20697 BegFim1A-like proteins belonging to the FimA/Mfa1 protein family (PDB code 4gpv) and could correspond to the stalk component of Bacteroidia type V pili. We could not identify candidates for accessory proteins to the putative BT3148-BT3147 pilus (Fig. 5 A and Fig. S4).

Based on these analyses, we hypothesized that BT3147 could be the major pilin of a structure exposed at the *B. thetaiotaomicron* cell surface. However, attempts to visualize BT3147-based pilus using immunofluorescence, and immuno-staining coupled to transmission electron microscopy analyses were unsuccessful, as it is sometimes the case for thin or masked fimbrial surface structures. Nevertheless, proteinase K sensitivity of BT3147 on treated whole cells suggested that this protein is surface exposed (Fig. S5)**.** We therefore tried tried to detect BT3147-containing structures by releasing *B. thetaiotaomicron* protruding surface appendages in the supernatant using a blender-based shaving procedure that do not lead to detectable bacterial lysis. We concentrated the protein obtained using this surface shaving procedure with strain VPI 5482 WT, *BT3147Δ9* Δ*BT3146-45*, class 1 transposon

mutant (2D7), and class 2 transposon mutant strain (1H2) and we performed an immunodetection using anti-BT3147 antibodies.

We detected BT3147 in all samples, with BT3147 truncated forms migrating lower than WT as described above (Fig. 5B and Fig. 4B). However, while WT displayed full length and monomeric protein, biofilm-forming *BT3147Δ9* Δ*BT3146-45* and 2D7 and 1H2 transposon mutants ample showed multiple specific products, potentially indicative of protein polymerization during pilus formation (Fig. 5B).

In vivo relevance of *BT3147*-mediated biofilm formation

The demonstration that BT3147 is exposed on *B. thetaiotaomicron* surface as part of a potential type V pilus structure contributing to *B. thetaiotaomicron* biofilm formation prompted us to investigate the *in vivo* role of BT3148-BT3147 to *B. thetaiotaomicron* adhesion or colonization. To this end, we used a germ-free mouse model of intestinal colonization and performed *in vivo* mixed cultures competition experiments, comparing the respective colonization capacity of the competing strains administrated intra-gastrically at a 1:1 mixed ratio ($2x10^7$ cells/ml). We first verified that *B. thetaiotaomicron ΔBT3146-3145* showed a similar colonization capacity than the wild type VPI 5482 strain indicating that deletion of *BT3146-3145* does not affect colonization (Fig. 6A). We then found that Δ*BT3148-BT3145* has the same colonization capacity as the wild type (Fig. 6B), and that the biofilm-forming strain *BT3147Δ9* Δ*BT3146-45* shows similar colonization capacity as the wild type VPI 5482 strain (Fig. 6C). This analysis therefore showed that BT3148-3147 putative pilus or its biofilm-promoting truncated form does not significantly contribute to *B. thetaiotaomicron* intestinal colonization capacity in the tested conditions.

DISCUSSION

In this study we investigated the biofilm formation capacity of the prominent gut symbiont *B. thetaiotaomicron*. We found that many *B. thetaiotaomicron* isolates displayed an increased biofilm formation capacity compared to the reference *B. thetaiotaomicron* VPI 5482 strain that is used in most gut microbiota studies. This widespread but highly variable capacity to form biofilm is observed in many aerobic bacteria, including the facultative anaerobe *Escherichia coli* (24) and *Staphylococcus epidermidis* (25) and is consistent with a study performed in *Bacteroides fragilis*, a closely related intestinal anaerobe, which also displays variable biofilm formation capacity (26). Biofilm formation by pathogenic bacteria is a major cause of chronic and recurring infections (2) and pathogenicity and abscess formation by *B. fragilis* is associated with biofilm and adhesion to peritoneal epithelium (27, 28). Whereas *B. thetaiotaomicron* usually behaves as an intestinal non-pathogenic bacterium, it is also found associated with abdominal and deep wound infections, representing up to 14% of the bacteria found at these sites (29). Since 5 out of 14 of the best biofilm-forming strains identified in our study were isolated from different infection sites (bone biopsies, blood samples, or abscesses, see Table S1), this suggests that biofilm formation of *B. thetaiotaomicron* could be correlated with opportunistic extra-intestinal infections and future investigations could provide insights into this aspect of *B. thetaiotaomicron* biology.

Our static and dynamic biofilm assays show that *B. thetaiotaomicron* strain VPI 5482 forms poor biofilms *in vitro*, which is consistent with the study performed by TerAvest and colleagues who obtained a VPI 5482 biofilm only after 8 days of continuous incubation in a chemostat (19). Whereas we did not observe significant biofilm accumulation in VPI 5482 even after 48h, this result might reflect the fact that VPI 5482 biofilm formation is repressed in laboratory conditions. For example, uropathogenic *E. coli* is known to cause infections by adhering to the bladder epithelium using fimbriae, but displays poor biofilm formation *in vitro* (30, 31). Similarly, Huang and colleagues demonstrated that *B. fragilis* poor adherence is enhanced on mucin-covered plates, which mimics the intestinal mucosa – the natural habitat of *B. fragilis* (32).

Our approach to uncover the biofilm potential and biofilm-related functions in *B. thetaiotaomicron* VPI 5482 resulted in the identification of two putative Mfa1-like proteins (BT3148 and BT3147) potentially involved in biofilm formation in *B. thetaiotaomicron.* BT3147 and BT3148 have N-terminal domain homologies with Mfa1 type pili of the closely related anaerobic oral pathogen *P. gingivalis*, in which two types of pili were described – the

long FimA and the short Mfa1, which represent the prototype of a recently defined type V pilus that are ubiquitous in gut bacteroidetes (20). In VPI 5482, genes *BT3148-3147* appear to encode a minimal Mfa1 type operon only encoding the potential pilus anchor (BT3148) and stalk pilin (BT3147) (Fig.5A). Intriguingly, studies of Mfa1-type pili in *P. gingivalis* showed that the presence of minor pilins is necessary for proper pili function and that deletion of the minor pili component *mfa4* results in complete loss of function (33, 34). The apparent lack of *mfa3-5* genes encoding accessory pilins near putative *mfa1*- and *mfa2*-like genes (*BT3147* and *BT3148* respectively) suggests that *BT3148-BT3147* might correspond to a new minimal type V pili operon that does not contain or lost its accessory pilins during evolution.

The contribution of the putative Mfa-like BT3148-BT3147-based pilus to biofilm formation is only revealed upon removal of the last 9 C-terminal amino acids of BT3147. The potential polymerization observed in our immune-detection experiments (Fig.5B) suggested that C-terminal truncation of the putative stalk pilin BT3147 could lead to the synthesis of an extended pilus, thus enhancing *in vitro* adhesion. This is surprising, as it has been suggested that the C-terminus plays a critical role in type V pili assembly (35) and the observed polymerization could correspond to an artifact introduced upon C-terminal truncation of BT3147. However, a similar phenotype had been described in *P. gingivalis*, in which deletion and truncation of the anchor resulted into the production of an unusually long pilus that promoted aggregation and biofilm formation (36, 37). The exact mechanism of synthesis of Mfa1 and FimA-like pili has not yet been resolved, however recent structural studies of crystal structures and cysteine-based crosslinking showed an interaction between beta strands of Mfa1 N- and C-termini (20, 35), indicating that polymerization could include a strand exchange between the C-terminal and N-terminal pilin domains (38). In *P. gingivalis*, maturation of Mfa1 pilins involves a N-terminus proteolytic cleavage step performed by RgpA/B arginine protease of *P. gingivalis*. The proteolysis takes place in a loop connecting two N-terminal ß-strands, enabling the removal of one strand, freeing a groove for the insertion of a C-terminal ß-strand coming from another Mfa1 pilin subunit. It is speculated that in this processive assembly process, Mfa1/FimA stalk pilin subunits need to undergo conformational changes allowing them to connect to the N-terminus of the next pilin unit (20). The critical role of the Mfa1/FimA C-terminus during type V pili assembly was recently confirmed by Hall and colleagues, as they showed that presence of the last 6 C-terminal amino acids is necessary for polymerization (35). The reason why truncation of the putative Mfa1-like *B. thetaiotaomicron* pilin BT3147 seems to stimulate rather than impair polymerization and biofilm formation is not clear but could reflect a structural difference in

the C-terminus of BT3147 compared to *P. gingivalis* Mfa1. We indeed could not find any homology associated with BT3147 C-terminus and the Mfa1-type structural model (pdb code 4gpv, Fig. S3). By contrast, Phyre structural model prediction of BT3147 suggests the presence of a long and unstructured C-terminus in BT3147 (Fig. S4). This suggests that at least some of *B. thetaiotaomicron* type V pilin structures might differ from *P. gingivalis* ones and could potentially require additional or different post-translational pili modifications during the assembly process. In our study, removing the last 9 C-terminal amino acids of BT3147 might have exposed the A1 C-terminal strand, that was shown to be involved in interaction with the N-terminus (35), allowing for pilus polymerization, as suggested by the polymerization pattern observed in the *BT3147Δ9* Δ*BT3146-45* strain (Figure 5B). In support of this possibility, we showed that BT3147Δ9 detected using anti-BT3147 antibodies migrates at about 10 kDa lower than the WT protein. We therefore hypothesize that the truncation in the BT3147Δ9 protein could unmask a protease cleavage site and undergo an extra proteolytic cleavage step. Preliminary results using mass spectrometry analysis of the shorter band detected in the 1H2 mutant indicated a protein size of 27 kDa, in accordance to the protein size observed by immunodetection and consistent with a further maturation of the protein.

Alternatively, considering that all type V pilins (major, minor and accessory) share domain homology in their N-termini, we cannot completely rule out that BT3147 belongs to the group of accessory pilins (Mfa3-5-like) whose C-terminal structure does not allow further pilus elongation (20). In this scenario, deletion of the last 9 C-terminal amino acids of BT3147 could remove a peptide normally blocking polymerization, thus resulting in the observed polymerization in the *BT3147Δ9 ΔBT3146-5* strain.

We could also show that *BT3147* is constitutively expressed in the wild type strain, suggesting that BT3148-BT3147 genes are not cryptic. However, as we were unable to see differences of colonization of the intestinal tract of germ-free mice using strains with WT or the mutated form of BT3147, the *in vivo* function of this locus is yet to be determined. In *P. gingivalis* the Mfa1 type filaments promote heterologous cell-to-cell interactions including adhesion to an oral pathogen often found in dental plaque *Streptococcus gordonii* (Lamont et al., 2002), and future work will determine whether a similar function is carried-out by *B. thetaiotaomicron* BT3148-BT3147.

Our study demonstrates the widespread ability of *B. thetaiotaomicron* to form biofilm and brings first evidence for the existence of functional type V pili structures as mediators of adhesion in *B. thetaiotaomicron in vitro.* We expect this work to contribute to the introduction

of *B. thetaiotaomicron* as a new a model to study proteinaceous adhesins and biofilm-related functions in intestinal colonization and microbiota-host interactions in this anaerobic gut symbiont.

MATERIALS AND METHODS

Bacterial strains and growth conditions

Bacterial strains used in this study are listed in Table S2. *B. thetaiotaomicron* was grown in BHIS broth (39) supplemented with erythromycin (20 µg/ml), tetracycline (2.5 µg/ml), gentamicin (200 µg/ml) or 5'-fluoro-2'-deoxyruidin (FdUR, 200 µg/ml) when required and incubated at 37°C in anaerobic conditions using anaerobic jars with anaerobic atmosphere generators or in a C400M Ruskinn anaerobic-microaerophilic station. *E. coli* S17λpir was grown in Lysogeny Broth (LB) broth supplemented with ampicillin (100 µg/ml) when required and incubated at 37°C. All media and chemicals were purchased from Sigma-Aldrich.

Biofilm formation in microfermenters

Continuous-flow biofilm microfermenters containing a removable glass spatula were used as described in (40) (see also https://research.pasteur.fr/en/tool/biofilm-microfermenters/), with or without internal bubbling of a filter-sterilized compressed mix of 90% nitrogen / 5% hydrogen /5% carbon dioxide (anaerobic biofilm conditions). Biofilm microfermenters were inoculated by placing the spatula in a culture solution adjusted to OD_{600}=0.5 (containing $2.5x10^8$ bacteria/ml) for 10 min. The spatula was then reintroduced into the microfermenter. Flow rate was then adjusted (30 ml/h) so that total time for renewal of microfermenter medium was lower than bacterial generation time, thus minimizing planktonic growth by constant dilution of non-biofilm bacteria.

Transposon mutagenesis and positive selection

We used pSAMbt – the previously published plasmid used for random mariner-based transposon mutagenesis (41), to generate a library of approximately 10.000 *B. thetaiotaomicron* mutants carrying erythromycin resistant transposons. The mutants were pooled and subjected to a positive selection procedure using biofilm microfermenters. The mutants pool was put in contact with the glass microfermenter spatula for 10 minutes and the spatula was then introduced in the microfermenter and incubated with internal bubbling agitation to select for the strongly adherent bacteria during 8 hours. Following incubation, the bacteria attached to the spatula were resuspended in 15 ml of fresh BHIS medium supplemented with erythromycin and incubated anaerobically overnight. On the next day the

overnight culture was used to start another round of positive selection. This procedure was repeated four times, with the last microfermenter incubation lasting 24 hours instead of 8 hours. The biofilm composed of adherent transposon mutants developing on the spatula was then recovered and plated out on BHIS-erythromycin agar to obtain single colonies that were then individually tested for biofilm formation using 96-well crystal violet staining.

Biofilm microtiter plate assay

Overnight cultures were diluted to OD_{600} = 0.01 ($5x10^6$ cells/ml) and inoculated in technical triplicates in a polystyrene Greiner 96-well plate. Incubation was done at 37°C in anaerobic conditions for 24 hours. Supernatant with free-floating bacteria was removed by careful pipetting and 100 µl of Bouin's solution (picric acid 0.9 %, formaldehyde 9 % and acetic acid 5 %) was applied during 15 minutes to fix the biofilm attached to the well. Next the fixation solution was washed 3 times with water and biofilm was stained with 1% crystal violet solution during 15 minutes. After removal of the crystal violet solution, biofilms were washed 3 times with water. For quantification of biofilm formation, dried stained biofilms were resuspended in a 1:5 acetone:ethanol mixture and absorbance was measured at 575 nm using a infinite M200 PRO plate reader. Biofilm formation in different *B. thetaiotaomicron* strains is represented in values normalized to average biofilm formation in the wild type VPI 5482.

Construction of B. thetaiotaomicron mutants

All experiments and genetic constructions of *B. thetaiotaomicron* were made in VPI 5482_Δ*tdk* strain, which was developed for 2-step selection procedure of unmarked gene deletion by allelic exchange, as previously described (42). Therefore, the VPI 5482_Δ*tdk* is referred to as wild type in this study. All primers used in this study are described in Table S3.

For the generation of deletion strains by allelic exchange in *B. thetaiotaomicron*, we used pExchange-*tdk* vector (42). Briefly, 1 Kb upstream and downstream regions of the target sequence were cloned in the pExchange-*tdk* vector and transformed into *E. coli* S17λpir strain that was used to deliver the vector to *B. thetaiotaomicron* by conjugation. Conjugation was carried out by mixing exponentially grown cultures of the donor and the recipient strain at a 2:1 ratio and mating was done by placing the mixture on Millipore 0.45 µm hydrophilic cellulose ester filter disc (ref. HAWP29325) on top of BHIS agar plates at 37°C in aerobic conditions over night. After this, bacteria were recovered by resuspending and vortexing the filters in fresh BHIS medium and then plated on selective BHIS agar supplemented with erythromycin for selection of *B. thetaiotaomicron* transconjugants that underwent the first

recombination event and gentamicin to ensure exclusion of any *E. coli* growth. Erythromycin and gentamicin-resistant colonies of *B. thetaiotaomicron* were then subjected to the second round of selection on BHIS agar plates supplemented with FdUR for selection of double recombination colonies. The resulting deletion mutants were confirmed by PCR and sequencing.

For gene constitutive expression we used the pNBU2-*bla-erm* vector (43), which inserts itself in the 5' untranslated region of the $tRNA^{ser}$, thus providing chromosomal based expression. In order to provide equal expression of different target genes we used the promoter of gene *BT1311* (coding for sigma factor RpoD), that had been cloned from a PCR fragment into the multiple cloning site of pNBU2-*bla-erm* to yield pNBU1311. Target genes were cloned (Start to Stop codon) using the NdeI/NotI sites of pNBU1311 and the resulting vector was then transformed into *E. coli* S17λpir strain. Transfer of the expression vector to *B. thetaiotaomicron* was done by conjugation as previously described, this time with only one selection step. The transformed *B. thetaiotaomicron* strains were selected on erythromycin and vector insertions were confirmed by PCR using pNBU1311-specific primers.

RNAseq analysis

Total RNA was extracted from exponentially grown cultures of the wild type *B. thetaiotaomicron* using MP Biomedicals FastRNA Pro™ BLUE KIT by the provider's manual and treated with Ambion Turbo DNA-free™ kit to remove possible DNA contamination. All samples were checked for residual genomic DNA contamination with the *DNAPol3*-F and *DNAPol3*-R primer pair (Table S3) and were considered DNA-free if no amplification was detected at <30 cycles. Ribosomal RNA was removed using Illumina Ribo-Zero™ rRNA Removal Kits and the purified RNA concentration was measured with NanoDrop and RNA quality was checked by Agilent 2100 BioAnalyzer. The obtained RNA samples were fragmented and used for cDNA library preparation using TruSeq Stranded mRNA Library Preparation Kit Set A™. Samples were sequenced with an Illumina HiSeq2500 sequencer. Sequence quality was analyzed by FastQC (https://www.bioinformatics.babraham.ac.uk/projects/fastqc/) and reads were aligned against the reference VPI 5482 genome using the Bowtie2 R package (44).

Structural analyses

CD-search analysis was performed using the CDSEARCH/cdd v3.15 database (45). 3D homology search was performed using Phyre2 program using the intensive mode (http://www.sbg.bio.ic.ac.uk/phyre2/html/page.cgi?id=index)

In vivo *mixed cultures competition experiments in germ-free mice*

Animal experiments were done at "Animalerie Axénique de MICALIS (ANAXEM)" platform (Microbiologie de l'Alimentation au Service de la Santé (MICALIS), Jouy-en-Josas, France) according to an official authorization n°3441-2016010614307552 delivered by a French ministry (Education nationale, enseignement supérieur et recherche). The protocol was approved by a local ethic committee on animal experimentation (committee n°45). All animals were housed in flexible-film isolators (Getinge-La Calhène, Vendôme, France) with controlled environment conditions (light/dark 12 h/12 h, temperature between 20 and 22°C, humidity between 45 to 55%). Mice were provided with sterile tap water and a gamma-irradiated standard diet (R03-40, S.A.F.E., Augy, France), ad libitum. Their bedding was composed of wood shavings and they were also given cellulose sheets as enrichment.

Methods: 6 male C3H/HeN germ free mice were gavaged with 200 µl bacterial suspensions containing 2x107 cell/ml consisting of 1:1 ratio mix of the wild type B. thetaiotaomicron and one of the tested strains: ΔBT3146-5, ΔBT3148-5 or BT3147Δ9_ΔBT3146-45. The wild type *B. thetaiotaomicron* carried erythromycin resistance gene (VPI 5482_pNBU2-bla-erm, Table S1) for later distinction from the erythromycin-sensitive tested strains. Six mice were used for each condition (wild-type with ΔBT3146-5, wild-type with ΔBT3148-5 and wild-type with BT3147Δ9_ΔBT3146-45). At 24, 48 and 96 hours after inoculation, feces were collected, homogenized in 1 ml of 1X PBS, and serial dilutions were plated onto BHIS agar plates with and without erythromycin (20 µg/ml). Intestinal colonization capacity of the wild type and different mutants was estimated by assessing their abundance in the feces using qPCR. Total bacterial DNA was isolated from the fecal samples with QIAamp® DNA Stool kit and 10 ng were used as template for qPCR amplification of gyrA and ermG using Brilliant II SYBR® Green QPCR Master Mix following the producer's manual. The reaction was performed in the BIORAD Thermal cycler and absolute quantities of target genes were determined using standard-curve quantification method. Gene copy number was calculated from the absolute quantities using the following formula: (Starting quantity ng * 60221 * 10^{23} molecules/mole) / (Amplicon length bp *660 g/mole * 1*10^{9} ng/g). The abundance of the wild type and the competing mutant strains was estimated by quantifying the copy number of genes coding for gyrase A subunit (*gyrA -BT0899*) and *ermG* conferring resistance to erythromycin. While

gyrA is present in the wild type as well as in the mutant strains, *ermG* is only present in the wild type strain. Therefore, the abundance of wild type strain corresponds to the copy number of *ermG* and the mutant strain abundance is deduced as difference in the copy number between *gyrA* (total population) and the *ermG* (wild type).

Statistical analysis

Unpaired two-tailed Mann-Whitney non parametric test analyses were performed using Prism 6.0 for Mac OS X (GraphPad Software, Inc.). Each experiment was performed at least 3 times. * $p<0.05$; ** $p<0.01$; *** $p<0.001$.

Generation of an antiserum against BT3147

Polyclonal antibodies against BT3147 were raised in rabbits injected with a mixture of two peptides: peptide 1: C-VYDETGKTEVKQETTF-coNH2 (corresponding to BT3147 amino acids 54-69) and peptide 2: C-VADGKTTGTESDTKT-coNH2 (corresponding to BT3147 amino acids 169-183). The design and synthesis of the peptides, as well as the production and purification of the antibody production were performed at the Covalab Research Institute, Villeurbane, France. A mix of peptide 1 and 2 with Freund adjuvant was used for immunization of rabbits by 3 intradermic injections at day 0, day 21 and day 42 of the immunization protocol, followed by a subcutaneous injection at day 74. At day 88 of the protocol anti-BT3147 antibodies were purified from rabbit serum using affinity chromatography with a mix of peptide 1 and 2 as column ligands.

Preparation of protein extracts from shaved bacteria

Overnight cultures in BHIS were washed and resuspended in 1X PBS. 'Shaving' of surface pili was performed as previously described (23). Briefly, 100 ml of culture was grown in BHIS for 48 h at 37°C without agitation in anaerobic conditions. The culture was centrifuged (6000 rpm, 10 min) and pellet resuspended in 1X PBS and potential surface appendages were 'shaved' on ice using a mini hand blender using 5 1-minute pulses (19 600 rpm). Next, the samples were centrifuged at 6000 rpm for 1h at 4°C and proteins from the supernatant were precipitated using 10% TCA for 48h at 4°C, followed by centrifugation at 20 000 rpm for 1h at 4°C. The pellet was washed with 100 % acetone and resuspended in 100 µl of 8M urea. 8 µg of 'shaved' surface protein was analyzed by western blot using anti-BT3147 antibodies.

Western blot analysis

Cultures were grown in BHIS overnight and 1 ml at $OD_{600=}2$ was centrifuged (7000 rpm for 5 min) and resuspended in 100µl of 1X Laemmli buffer with 250U of benzonase nuclease (Sigma E0114) and incubated for 5 minutes at 95°C. Aliquots of these raw cell extracts or protein extract from shaved bacteria were run on Mini-PROTEAN TGX Stain-Free™ precast Gels (BioRad) in 1X TGX buffer and then transferred to nitrocellulose membrane using a Trans-Blot® Turbo™ Transfer System (BioRad). Blocking was performed during 1 h in a 5% solution of dry milk and 0.05% Tween –1X PBS (1X PBST). The membranes were then incubated overnight in 1X PBST with anti-BT3147 antiserum at 1:1000 at 4°C with agitation. Membranes were washed in 1X PBST and then incubated with the secondary antibody (anti-rabbit IgG conjugated with horse radish peroxidase at 1:3000, Promega). After washing the excess second antibody, specific bands were visualized using the ECL prime detection method (GE Healthcare).

COMPETING FINANCIAL INTERESTS

The authors declare no competing financial interests.

ACKNOWLEDGEMENTS.

We thank Andy Goodman and Justin Sonnenburg for generously providing plasmids and strains used as genetic tools in this study, Marie-Cécile Ploy, Luc Dubreuil for providing *B. thetaiotaomicron* strains and Bruno Dupuy and Isabelle Martin-Verstraete for their help and advice regarding the handling of anaerobic bacteria. This work was supported by an Institut Pasteur grant and by the French government's Investissement d'Avenir Program, Laboratoire d'Excellence "Integrative Biology of Emerging Infectious Diseases" (grant n°ANR-10-LABX-62-IBEID) and the *Fondation pour la Recherche Médicale* (grant no. DEQ20180339185 Equipe FRM 2018). J. Mihajlovic was supported by the Pasteur Paris University International Doctoral Program and the *Fondation pour la Recherche Médicale* (grant no. FDT20160435523).

REFERENCES

1. Hall-Stoodley L, Costerton JW, Stoodley P. 2004. Bacterial biofilms: from the natural environment to infectious diseases. Nature Reviews Microbiology 2:95-108.
2. Lebeaux D, Ghigo J-M, Beloin C. 2014. Biofilm-related infections: bridging the gap between clinical management and fundamental aspects of recalcitrance toward antibiotics. Microbiology and molecular biology reviews: MMBR 78:510-543.
3. Reyes M, Borras L, Seco A, Ferrer J. 2015. Identification and quantification of microbial populations in activated sludge and anaerobic digestion processes. Environ Technol 36:45-53.
4. Arumugam M, Raes J, Pelletier E, Le Paslier D, Yamada T, Mende DR, Fernandes GR, Tap J, Bruls T, Batto J-M, Bertalan M, Borruel N, Casellas F, Fernandez L, Gautier L, Hansen T, Hattori M, Hayashi T, Kleerebezem M, Kurokawa K, Leclerc M, Levenez F, Manichanh C, Nielsen HB, Nielsen T, Pons N, Poulain J, Qin J, Sicheritz-Ponten T, Tims S, Torrents D, Ugarte E, Zoetendal EG, Wang J, Guarner F, Pedersen O, de Vos WM, Brunak S, Doré J, Meta HITC, Antolín M, Artiguenave F, Blottiere HM, Almeida M, Brechot C, Cara C, Chervaux C, Cultrone A, Delorme C, Denariaz G, et al. 2011. Enterotypes of the human gut microbiome. Nature 473:174-180.
5. Rajilić-Stojanović M, Vos D, M W. 2014. The first 1000 cultured species of the human gastrointestinal microbiota. FEMS Microbiology Reviews 38:996-1047.
6. Sonnenburg JL, Angenent LT, Gordon JI. 2004. Getting a grip on things: how do communities of bacterial symbionts become established in our intestine? Nature Immunology 5:569-573.
7. Palestrant D, Holzknecht ZE, Collins BH, Parker W, Miller SE, Bollinger RR. 2004. Microbial biofilms in the gut: visualization by electron microscopy and by acridine orange staining. Ultrastructural Pathology 28:23-27.

8. Swidsinski A, Loening-Baucke V, Lochs H, Hale L-P. 2005. Spatial organization of bacterial flora in normal and inflamed intestine: a fluorescence in situ hybridization study in mice. World Journal of Gastroenterology 11:1131-1140.

9. Macfarlane S, Dillon JF. 2007. Microbial biofilms in the human gastrointestinal tract. Journal of Applied Microbiology 102:1187-1196.

10. Dejea CM, Wick EC, Hechenbleikner EM, White JR, Mark Welch JL, Rossetti BJ, Peterson SN, Snesrud EC, Borisy GG, Lazarev M, Stein E, Vadivelu J, Roslani AC, Malik AA, Wanyiri JW, Goh KL, Thevambiga I, Fu K, Wan F, Llosa N, Housseau F, Romans K, Wu X, McAllister FM, Wu S, Vogelstein B, Kinzler KW, Pardoll DM, Sears CL. 2014. Microbiota organization is a distinct feature of proximal colorectal cancers. Proc Natl Acad Sci U S A 111:18321-6.

11. Johnson CH, Dejea CM, Edler D, Hoang LT, Santidrian AF, Felding BH, Ivanisevic J, Cho K, Wick EC, Hechenbleikner EM, Uritboonthai W, Goetz L, Casero RA, Jr., Pardoll DM, White JR, Patti GJ, Sears CL, Siuzdak G. 2015. Metabolism links bacterial biofilms and colon carcinogenesis. Cell Metab 21:891-7.

12. Xu J, Bjursell MK, Himrod J, Deng S, Carmichael LK, Chiang HC, Hooper LV, Gordon JI. 2003. A genomic view of the human-Bacteroides thetaiotaomicron symbiosis. Science (New York, NY) 299:2074-2076.

13. Hooper LV, Wong MH, Thelin A, Hansson L, Falk PG, Gordon JI. 2001. Molecular analysis of commensal host-microbial relationships in the intestine. Science (New York, NY) 291:881-884.

14. Hooper LV, Stappenbeck TS, Hong CV, Gordon JI. 2003. Angiogenins: a new class of microbicidal proteins involved in innate immunity. Nature Immunology 4:269-273.

15. Zocco MA, Ainora ME, Gasbarrini G, Gasbarrini A. 2007. Bacteroides thetaiotaomicron in the gut: molecular aspects of their interaction. Digestive and Liver

Disease: Official Journal of the Italian Society of Gastroenterology and the Italian Association for the Study of the Liver 39:707-712.

16. Martens EC, Koropatkin NM, Smith TJ, Gordon JI. 2009. Complex glycan catabolism by the human gut microbiota: the Bacteroidetes Sus-like paradigm. The Journal of Biological Chemistry 284:24673-24677.

17. Viljanen MK, Linko L, Lehtonen OP. 1988. Detection of Bacteroides fragilis, Bacteroides thetaiotaomicron, and Bacteroides ovatus in clinical specimens by immunofluorescence with a monoclonal antibody to B. fragilis lipopolysaccharide. Journal of Clinical Microbiology 26:448-452.

18. Feuillet L, Carvajal J, Sudre I, Pelletier J, Thomassin JM, Drancourt M, Cherif AA. 2005. First isolation of Bacteroides thetaiotaomicron from a patient with a cholesteatoma and experiencing meningitis. Journal of Clinical Microbiology 43:1467-1469.

19. TerAvest MA, He Z, Rosenbaum MA, Martens EC, Cotta MA, Gordon JI, Angenent LT. 2014. Regulated expression of polysaccharide utilization and capsular biosynthesis loci in biofilm and planktonic Bacteroides thetaiotaomicron during growth in chemostats. Biotechnology and Bioengineering 111:165-173.

20. Xu Q, Shoji M, Shibata S, Naito M, Sato K, Elsliger M-A, Grant JC, Axelrod HL, Chiu H-J, Farr CL, Jaroszewski L, Knuth MW, Deacon AM, Godzik A, Lesley SA, Curtis MA, Nakayama K, Wilson IA. 2016. A Distinct Type of Pilus from the Human Microbiome. Cell 165:690-703.

21. Yoshimura F, Murakami Y, Nishikawa K, Hasegawa Y, Kawaminami S. 2009. Surface components of Porphyromonas gingivalis. Journal of Periodontal Research 44:1-12.

22. Nagano K, Hasegawa Y, Abiko Y, Yoshida Y, Murakami Y, Yoshimura F. 2012. Porphyromonas gingivalis FimA Fimbriae: Fimbrial Assembly by fimA Alone in the fim Gene Cluster and Differential Antigenicity among fimA Genotypes. PLoS ONE 7.
23. Larsonneur F, Martin FA, Mallet A, Martinez-Gil M, Semetey V, Ghigo J-M, Beloin C. 2016. Functional analysis of Escherichia coli Yad fimbriae reveals their potential role in environmental persistence. Environmental Microbiology 18:5228-5248.
24. Mansan-Almeida R, Pereira AL, Giugliano LG. 2013. Diffusely adherent Escherichia coli strains isolated from children and adults constitute two different populations. BMC microbiology 13:22.
25. Begovic J, Jovcic B, Papic-Obradovic M, Veljovic K, Lukic J, Kojic M, Topisirovic L. 2013. Genotypic diversity and virulent factors of Staphylococcus epidermidis isolated from human breast milk. Microbiol Res 168:77-83.
26. Reis ACM, Silva JO, Laranjeira BJ, Pinheiro AQ, Carvalho CBM. 2014. Virulence factors and biofilm production by isolates of Bacteroides fragilis recovered from dog intestinal tracts. Brazilian Journal of Microbiology 45:647-650.
27. Chung DR, Kasper DL, Panzo RJ, Chitnis T, Grusby MJ, Sayegh MH, Tzianabos AO, Chtinis T. 2003. CD4+ T cells mediate abscess formation in intra-abdominal sepsis by an IL-17-dependent mechanism. Journal of Immunology (Baltimore, Md: 1950) 170:1958-1963.
28. Gibson FC, Onderdonk AB, Kasper DL, Tzianabos AO. 1998. Cellular mechanism of intraabdominal abscess formation by Bacteroides fragilis. Journal of Immunology (Baltimore, Md: 1950) 160:5000-5006.
29. Brook I. 1989. Pathogenicity of the Bacteroides fragilis group. Annals of Clinical and Laboratory Science 19:360-376.

30. Eto DS, Jones TA, Sundsbak JL, Mulvey MA. 2007. Integrin-mediated host cell invasion by type 1-piliated uropathogenic Escherichia coli. PLoS pathogens 3:e100.
31. Valle J, Da Re S, Henry N, Fontaine T, Balestrino D, Latour-Lambert P, Ghigo JM. 2006. Broad-spectrum biofilm inhibition by a secreted bacterial polysaccharide. Proc Natl Acad Sci U S A 103:12558-63.
32. Huang JY, Lee SM, Mazmanian SK. 2011. The human commensal Bacteroides fragilis binds intestinal mucin. Anaerobe 17:137-141.
33. Ikai R, Hasegawa Y, Izumigawa M, Nagano K, Yoshida Y, Kitai N, Lamont RJ, Yoshimura F, Murakami Y. 2015. Mfa4, an Accessory Protein of Mfa1 Fimbriae, Modulates Fimbrial Biogenesis, Cell Auto-Aggregation, and Biofilm Formation in Porphyromonas gingivalis. PloS One 10:e0139454.
34. Zheng C, Wu J, Xie H. 2011. Differential expression and adherence of Porphyromonas gingivalis FimA genotypes. Molecular Oral Microbiology 26:388-395.
35. Hall M, Hasegawa Y, Yoshimura F, Persson K. 2018. Structural and functional characterization of shaft, anchor, and tip proteins of the Mfa1 fimbria from the periodontal pathogen Porphyromonas gingivalis. Sci Rep 8:1793.
36. Hasegawa Y, Iwami J, Sato K, Park Y, Nishikawa K, Atsumi T, Moriguchi K, Murakami Y, Lamont RJ, Nakamura H, Ohno N, Yoshimura F. 2009. Anchoring and length regulation of Porphyromonas gingivalis Mfa1 fimbriae by the downstream gene product Mfa2. Microbiology 155:3333-3347.
37. Nagano K, Hasegawa Y, Murakami Y, Nishiyama S, Yoshimura F. 2010. FimB regulates FimA fimbriation in Porphyromonas gingivalis. Journal of Dental Research 89:903-908.

712 38. Lee JY, Miller DP, Wu L, Casella CR, Hasegawa Y, Lamont RJ. 2018. Maturation of
713 the Mfa1 Fimbriae in the Oral Pathogen Porphyromonas gingivalis. Front Cell Infect
714 Microbiol 8:137.
715 39. Bacic MK, Smith CJ. 2008. Laboratory maintenance and cultivation of bacteroides
716 species. Current Protocols in Microbiology Chapter 13:Unit-13C.1.
717 40. Ghigo JM. 2001. Natural conjugative plasmids induce bacterial biofilm development.
718 Nature 412:442-445.
719 41. Goodman AL, McNulty NP, Zhao Y, Leip D, Mitra RD, Lozupone CA, Knight R,
720 Gordon JI. 2009. Identifying genetic determinants needed to establish a human gut
721 symbiont in its habitat. Cell Host & Microbe 6:279-289.
722 42. Koropatkin NM, Martens EC, Gordon JI, Smith TJ. 2008. Starch catabolism by a
723 prominent human gut symbiont is directed by the recognition of amylose helices.
724 Structure (London, England : 1993) 16:1105-1115.
725 43. Wang J, Shoemaker NB, Wang G-R, Salyers AA. 2000. Characterization of a
726 Bacteroides Mobilizable Transposon, NBU2, Which Carries a Functional Lincomycin
727 Resistance Gene. Journal of Bacteriology 182:3559-3571.
728 44. Langmead B, Salzberg SL. 2012. Fast gapped-read alignment with Bowtie 2. Nat
729 Methods 9:357-9.
730 45. Marchler-Bauer A, Derbyshire MK, Gonzales NR, Lu S, Chitsaz F, Geer LY, Geer
731 RC, He J, Gwadz M, Hurwitz DI, Lanczycki CJ, Lu F, Marchler GH, Song JS, Thanki
732 N, Wang Z, Yamashita RA, Zhang D, Zheng C, Bryant SH. 2015. CDD: NCBI's
733 conserved domain database. Nucleic Acids Res 43:D222-6.
734
735
736
737

FIGURE AND FIGURE LEGENDS

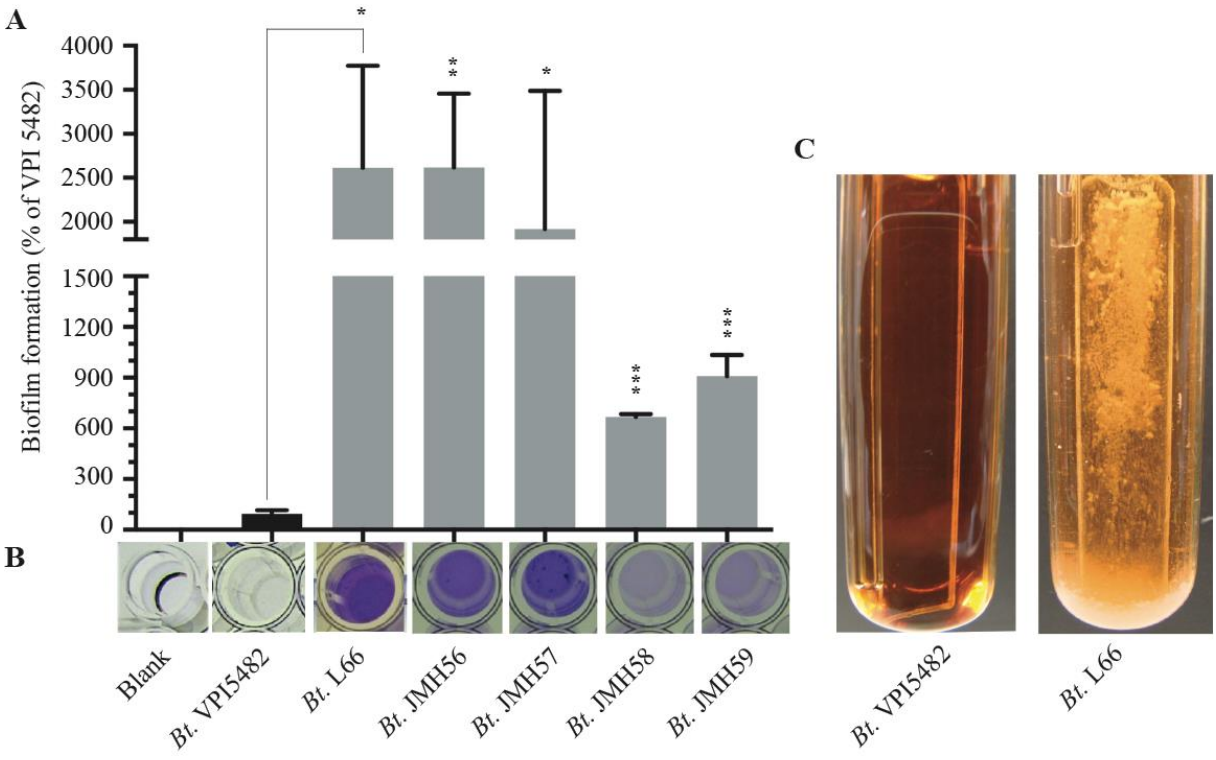

Figure 1. *B. thetaiotaomicron* VPI 5482 strain forms poor biofilms compared to different isolates. **A-B**. Biofilm formation in 96-well plate biofilm assay followed by crystal violet staining of *B. thetaiotaomicron* VPI 5482 and various biofilm-forming *B. thetaiotaomicron* isolates (see also Supplementary Figure S1). Error bars indicate standard deviation of 3 technical replicates. * $p<0.05$; ** $p<0.01$; *** $p<0.001$. **C**. Biofilm formation on a glass slide inserted in continuous-flow biofilm microfermenters. The images were taken 48 h after inoculation.

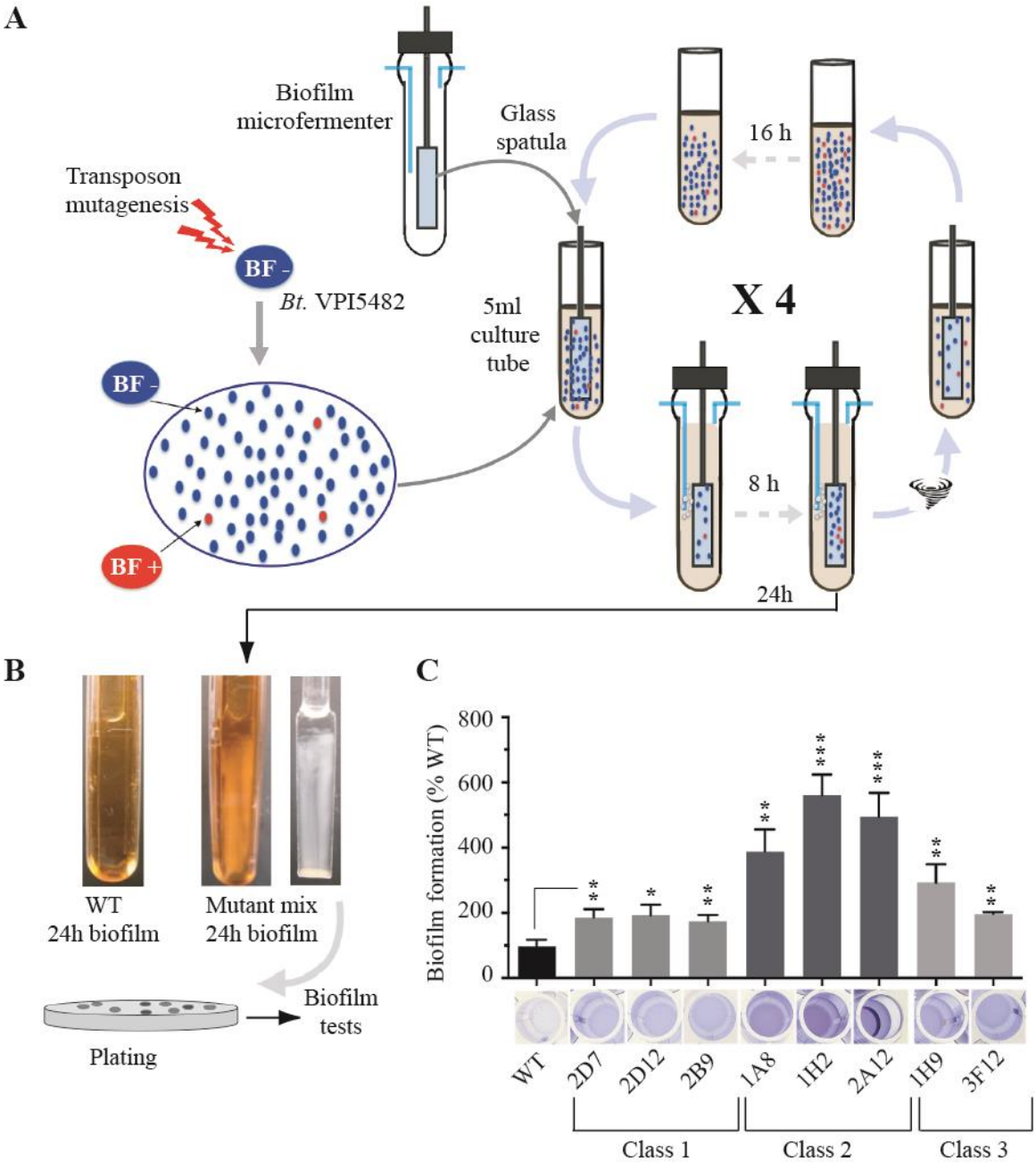

Figure 2. Selection of *B. thetaiotaomicron* VPI 5482 mutants with increased biofilm capacities. A Schematic representation of the positive selection strategy used to identify transposon mutants with an increased biofilm production. **B** Biofilm biomass formation on the internal spatula of continuous-flow biofilm microfermenters after 24 h. On the left, wild type *B. thetaiotaomicron* VPI 5482, in the middle and on the right: microfermenter and spatula inoculated with a culture enriched for biofilm production after 4 cycles of positive selection. **C** Comparison of the biofilm formation capacity of *B. thetaiotaomicron* WT and eight identified mutants with insertion in gene *BT3147* Bottom: crystal violet staining in 96-well microtiter plates. Top: corresponding biomass quantification after resuspension in acetone:ethanol mix and absorbance measured at 575 nm . Biofilm formation capacities of WT (VPI 5482) have been set to 100%. Error bars indicate standard deviation of 3 technical replicates. * $p<0.05$; ** $p<0.01$; *** $p<0.001$.

763

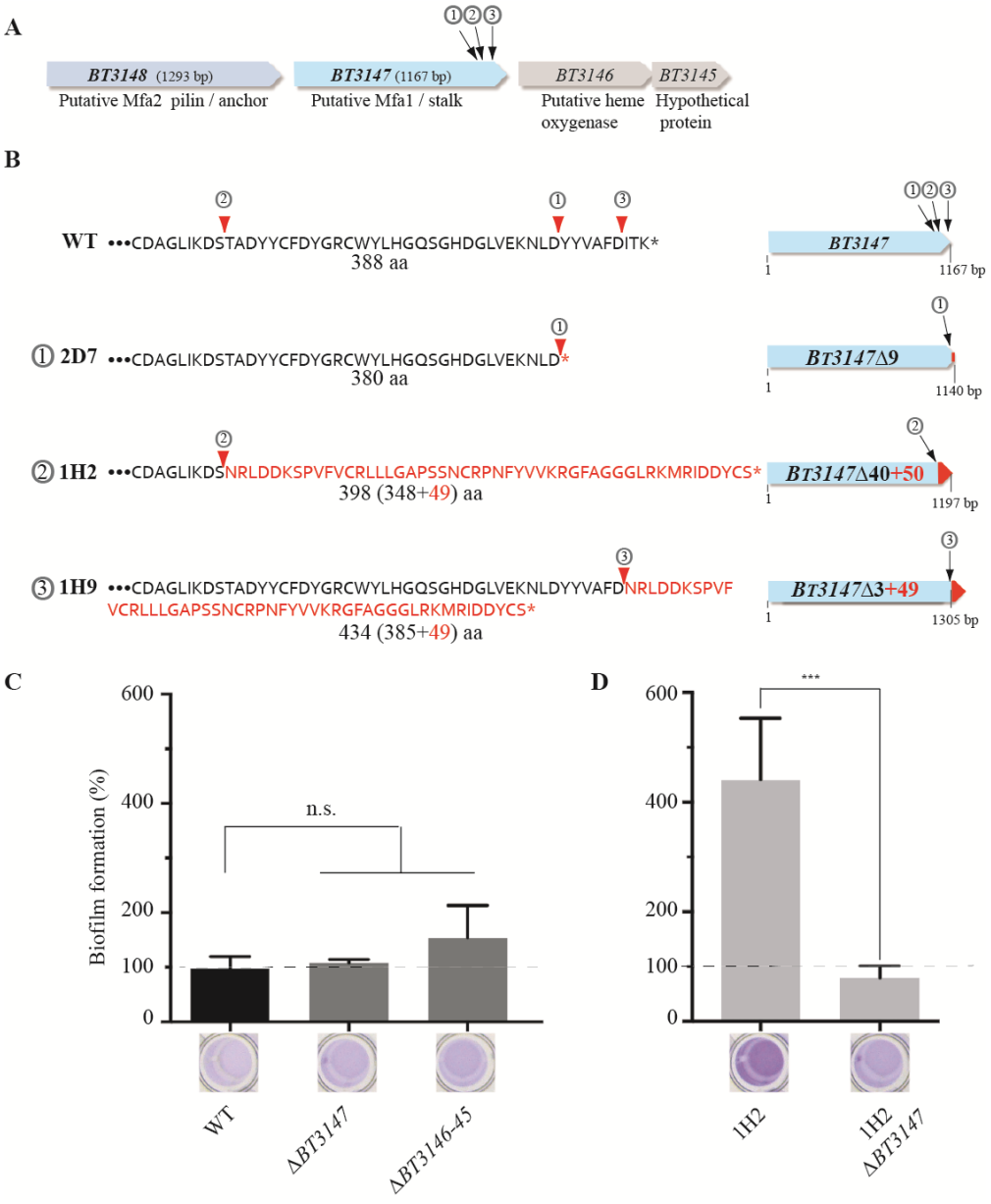

Figure 3.Insertions of transposon in the 3'-end of *B. thetaiotaomicron BT3147* increase biofilm formation A. Genetic organization of the *BT3148-3145 B. thetaiotaomicron* locus with indication of the three transposon insertion points in the 3' end of *BT3147*. 2D7 corresponds to class 1 (①) mutants. 1H2 corresponds to class 2 (②) mutant. 1H9 corresponds to class 3 (③) mutant. **B.** Schematic representation of the genetic consequences of transposon insertion in *BT3147*. **C.** Comparison of biofilm formation capacity of *B. thetaiotaomicron* WT (VPI 5482) with class 2 transposon mutant 1H2 and different deletion strains lacking either BT3147 (*ΔBT3147*), BT3146 and BT3145 (*ΔBT3146-45*). Bottom: crystal violet staining in 96-well microtiter plates. Top: corresponding quantification after resuspension in acetone:ethanol and absorbance measured at 575 nm **D.** Comparison of biofilm formation capacity *B. thetaiotaomicron* 1H2 mutant and strain 1H2*ΔBT3147*, derived from the biofilm-forming 1H2 transposon mutant after deletion of *BT3147* 1046 bp located upstream of the transposon insertion. Biofilm formation capacities of WT (VPI 5482) have been set to 100%. Error bars indicate standard deviation of 3 technical replicates. * $p<0.05$; ** $p<0.01$; *** $p<0.001$.

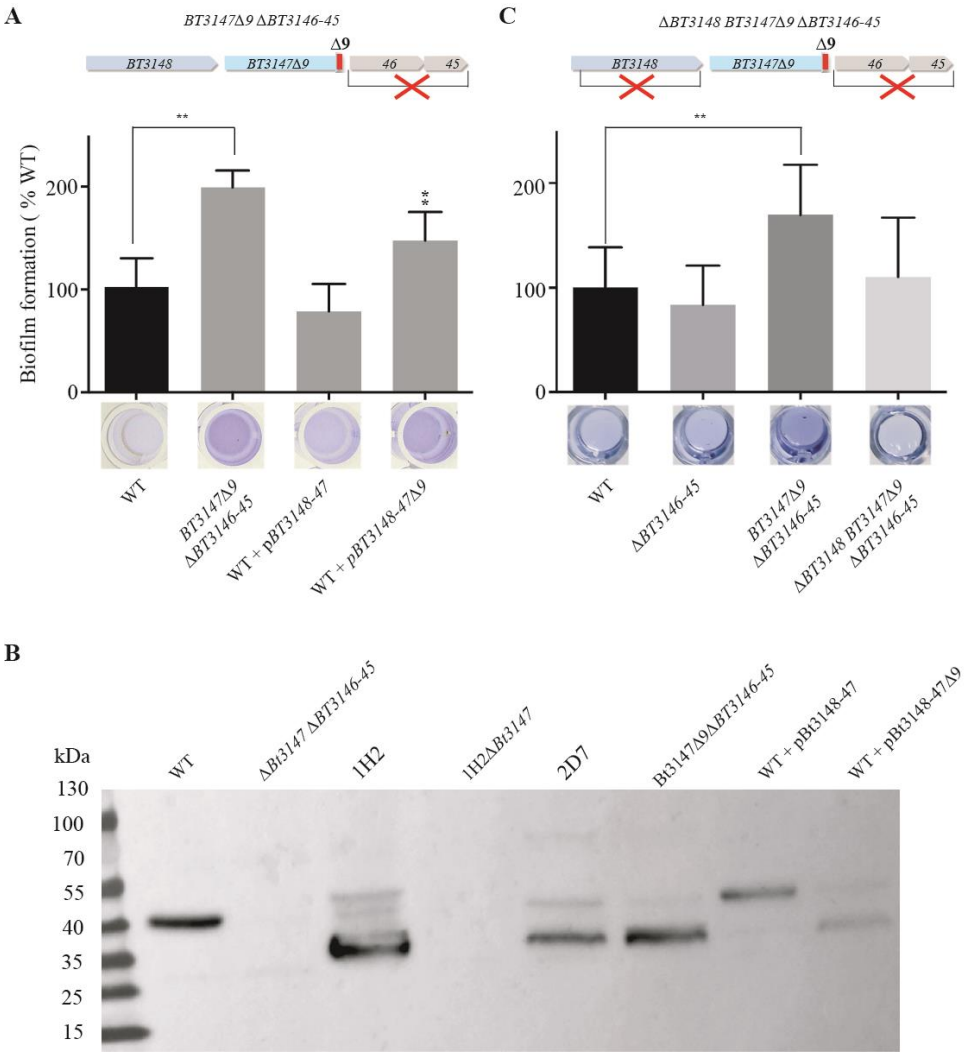

Figure 4. C-terminal truncation of BT3147 protein promotes *B. thetaiotaomicron* biofilm formation. A. Top, schematic genetic organization of the *BT3147Δ9 ΔBT3146-45* mutant. Bottom: comparison of the biofilm formation of WT *B. thetaiotaomicron* VPI 5482 and indicated mutant or plasmid-containing strains. Bottom: crystal violet staining in 96-well microtiter plates. Top: corresponding quantification after resuspension in acetone:ethanol and absorbance measured at 575 nm. Biofilm formation capacities of WT (VPI 5482) have been set to 100%. Error bars indicate standard deviation of 3 technical replicates. * $p<0.05$; ** $p<0.01$; *** $p<0.001$. **B.** Immunodetection of BT3147 in WT *B. thetaiotaomicron* VPI 5482 and indicated mutants or complemented strains expressing either full length BT3147 (p.*BT3148-7*) or truncated version of BT3147..

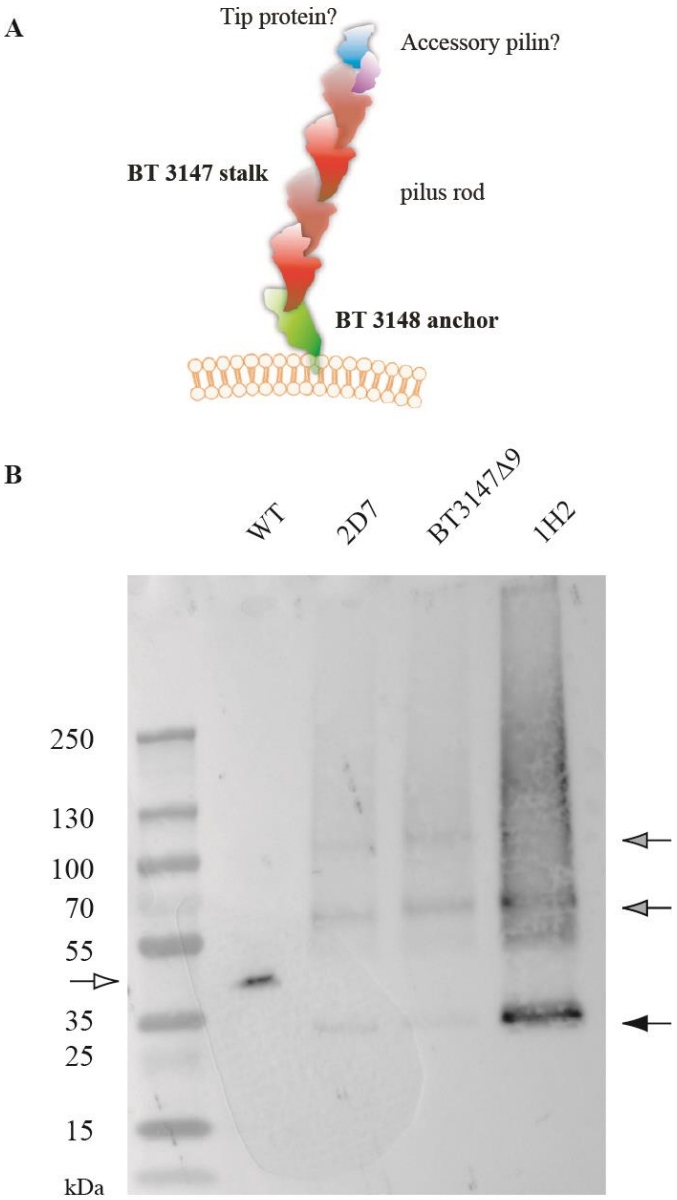

Figure 5. BT3147 is exposed on *B. thetaiotaomicron* surface as part of a potential type V pilus.

A. Model of the putative BT3148-7 pilus. **B.** Western blot analysis of BT3147-containing structures released after surface shaving of the indicated *B. thetaiotaomicron* strains and mutants, followed by immunodetection using anti-BT3147 antibodies. White arrows indicates WT, black arrows indicate BT3147Δ9 variant of BT3147 and its potential multimers.

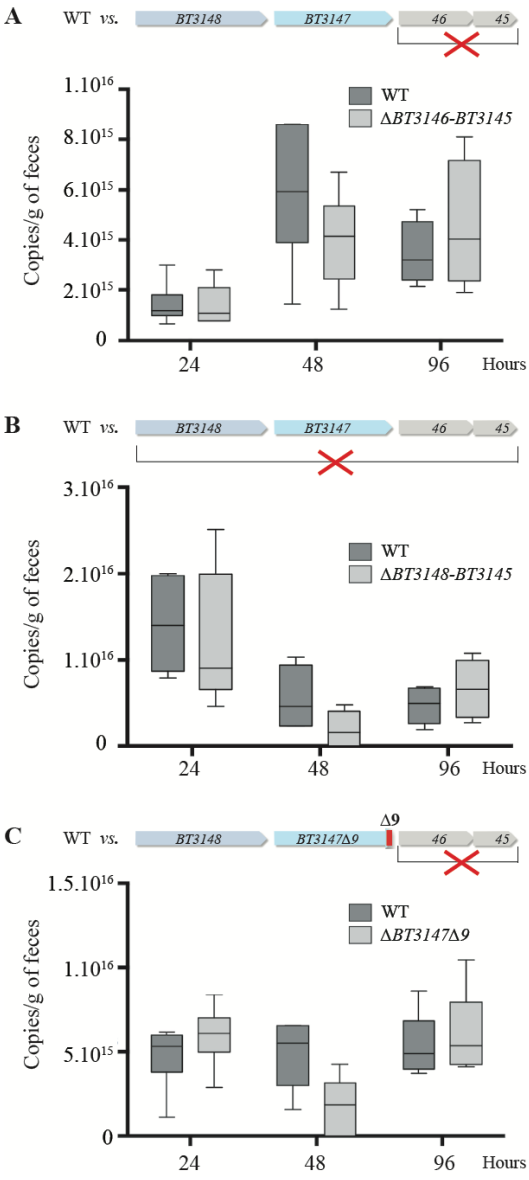

Figure 6. Contribution of genes *BT3148-5* to *B. thetaiotaomicron in vivo* intestinal colonization in germ-free mice. **A**: *in vivo* mixed cultures competition experiments, comparing the respective colonization capacity of WT and *ΔBT3146-BT3145* strains. **B**: *in vivo* mixed cultures competition experiments, comparing the respective colonization capacity of WT and *ΔBT3148-BT3145* strain. **C**: *in vivo* mixed cultures competition experiments, comparing the respective colonization capacity of WT and the biofilm-forming *BT3147Δ9 BT3146-BT3145* strain. All strains were administrated intra-gastrically at 1:1 mixed ratio ($2x10^7$ cell/ml). Comparisons were performed after collecting feces samples at 24 h, 48 h, and 96 h after the initial gavage and strain-specific qPCR on frozen fecal material samples and did not show any significant statistical difference between the tested strains.

SUPPLEMENTARY MATERIAL

SUPPLEMENTARY FIGURES

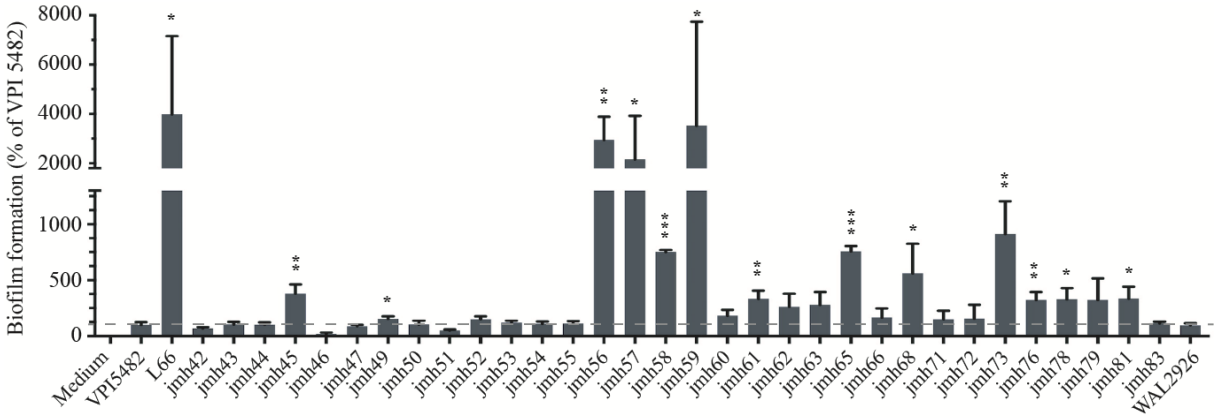

Supplementary Figure S1. **Biofilm formation by 34 *B. thetaiotaomicron* natural isolates**. Comparison of biofilm formation in various *B. thetaiotaomicron* isolates in a 96-well plate biofilm assay followed by crystal violet staining. VPI 5482 biofilm formation has been set to 100% as represented by the grey dashed lines and used for reference in the statistical test. These strains were collected from adults by the Microbiology laboratory of Dupuytren (Limoges) and Dron Tourcoing (Tourcoing) hospitals in France. For a complete list of the strains, see supplementary Table S3. Error bars indicate standard deviation of 3 technical replicates. * $p<0.05$; ** $p<0.01$; *** $p<0.001$.

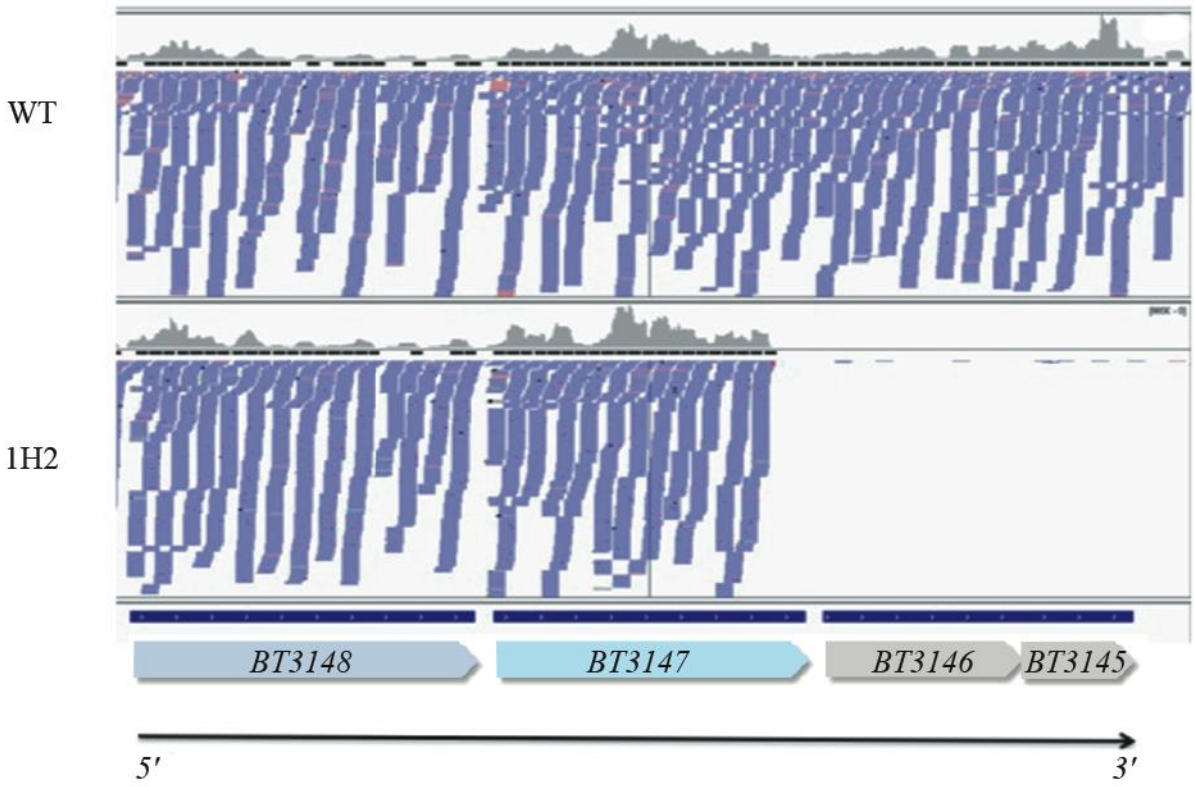

Supplementary Figure S2. Transcription in *BT3148-5* locus in WT *B. thetaiotaomicron* VPI 5482 and the transposon mutant 1H2. Reads mapping in the *BT3148-5* region are represented in blue, antisense reads are represented in red. Strand-specific mapping shows no antisense transcripts arising from the *BT3146-5* towards *BT3147*. *BT3147* transcript is uninterrupted in the WT indicating that there are no premature stop codons or transcription-stopping secondary structures. Transcription of the last portion of *BT3147* (position 1047 to 1167 bp) and *BT3146-5* is abolished in 1H2 due to transposon insertion.

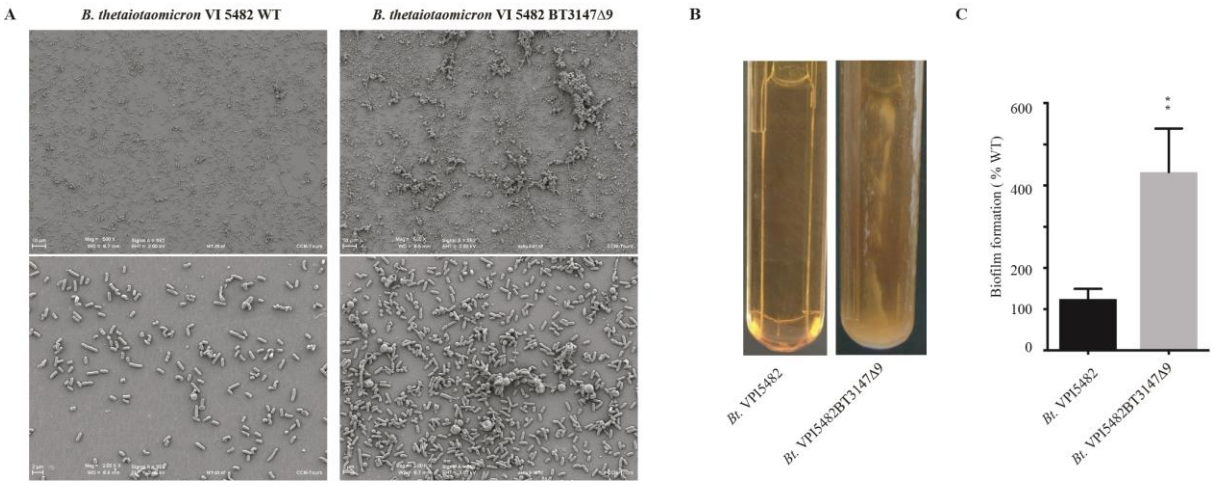

Supplementary Figure S3. C-terminal truncation of **BT3147 increases *in vitro* adhesion and biofilm formation. A** Scanning electron microscopy observation of *B. thetaiotaomicron* WT and *BT3147Δ9* grown in continuous flow biofilm-microfermenter (x500 and x2000 magnification) **B** Biofilm formation *B. thetaiotaomicron* WT and *BT3147Δ9* on a glass slide inserted in continuous flow biofilm microfermenters. The images were taken 48h after inoculation. **B** Quantification after resuspension and measure at OD 600 of *B. thetaiotaomicron* WT and *BT3147Δ9* in continuous flow biofilm microfermenters after 48h.

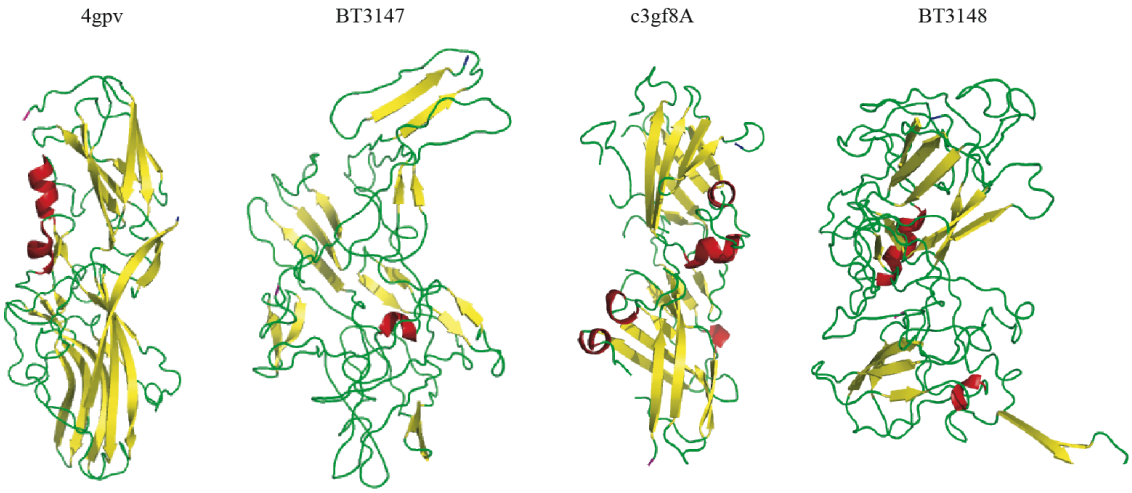

Supplementary Figure S4. Comparison of structural models of BT3147 and BT3148. Structural modeling for BT3147 and BT3148 has been performed using Phyre2 web interface with the intensive mode (http://www.sbg.bio.ic.ac.uk/phyre2/html/page.cgi?id=index) and compared to 3D-structure of Mfa1-type structural model (PDB code 4gpv:) and Fim2B/Mfa2 structural model (PDB code c3gf8A).

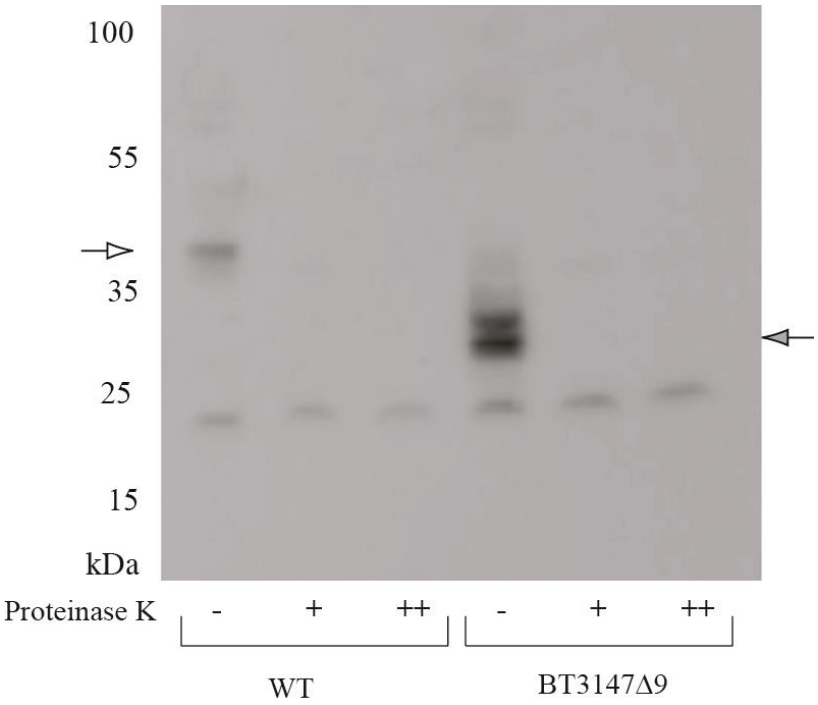

Supplementary Figure S5. BT3147 sensitivity to proteinaseK treatment on whole-cells Whole cells were washed with Tris 50mM pH 8.8 washed and treated with 10 µg/ml or 20 µg/ml proteinase K for 30 minutes at 37°C. This treatment leads to degradation of BT3147 and disparition of BT3147 signal. White arrows indicates WT BT3147, black arrows indicate BT3147Δ9 variant.

869 **SUPPLEMENTARY TABLES**

870

871 **Table S1. Wild type *B. thetaiotaomicron* collection used in this study**

Strains and plasmids	Relevant characteristics	References
Bacteroides thetaiotaomicron		
VPI 5482	Healthy adult human feces	(1)
L66	Healthy adult human feces, INRA	INRA
Jmh 42	Perforated ulcer	CHU Limoges
Jmh 43	Blood	CHU Limoges
Jmh 44	Blood	CHU Limoges
Jmh 45	Liquid from redon drain	CHU Limoges
Jmh 46	Blood	CHU Limoges
Jmh 47	Hepatic abscess	CHU Limoges
Jmh 48	Abscess	CHU Limoges
Jmh 49	Blood	CHU Limoges
Jmh 50	Liquid ascite	CHU Limoges
Jmh 51	Blood	CHU Limoges
Jmh 52	Blood	CHU Limoges
Jmh 53	Peritoneal liquid	CHU Limoges
Jmh 54	Bone biopsy	CHU Limoges
Jmh 55	Skin biopsy	CHU Limoges
Jmh 56	Blood	CHU Limoges
Jmh 57	Bone biopsy	CHU Limoges
Jmh 58	Blood	CHU Limoges
Jmh 59	Blood	CHU Limoges
Jmh 60	Hip implant	CHU Limoges
Jmh 61	DPCA	CHU Limoges
Jmh 62	Peritoneal liquid	CHRU Lille
Jmh 63	Blood	CHRU Lille

Jmh 65	Abdomen	CHRU Lille
Jmh 66	Maxilar pus	CHRU Lille
Jmh 68	Blood	CHRU Lille
Jmh 71	Blood	CHRU Lille
Jmh 72	Anal abscess	CHRU Lille
Jmh 73	Blood	CHRU Lille
Jmh 76	Fat tissue	CHRU Lille
Jmh 78	Abdominal abscess	CHRU Lille
Jmh 79	Intestinal cyste	CHRU Lille
Jmh 81	Blood	CHU Limoges
Jmh 83	Peritoneal liquid	CHRU Lille

1. Xu J, Bjursell MK, Himrod J, Deng S, Carmichael LK, Chiang HC, Hooper LV, Gordon JI. 2003. A genomic view of the human-Bacteroides thetaiotaomicron symbiosis. Science (New York, NY) 299:2074-2076.

879

880 **TABLE S2. Primers used in this study.**

Strain construction and analysis	Name	Sequence
Δ*BT3147*	*BT3147*-up-F	5'-GCGGTCGACAATGTGACGGAG GACGGCATCAGC-3'
	BT3147-up-R	5'-CAAAAAAACTTTTTTAATCATTTTCTAATTG-3'
	BT3147-down-F	5'-CGAATGGAGCGGAATATACAATGTGTGGATA ATCATGCGTGGACGGAGTATCC-3'
	BT3147-down-R	5'-GCGTCTAGATGAGCCGATGCAACTGTTG GTTGC-3'
Δ*BT3146-5*	*BT3146*-up-F	5'-GCGGTCGACTTTCGAAAACAACTGCTTTACC-3'
	BT3146-up-R	5'-AATTGTTTACGTTTAAAATTATTGAATGTGTC-3'
	BT3145-down-F	5'-GACACATTCAATAATTTTAAACGTAAACA ATTATTGAAAAAAAACAAGCTAGG-3'
	BT3145-down-R	5'-CCCGCGGCCGCCTACGGCACAGTTGA GAGATTGGAG-3'
*BT3147*Δ*9*	*BT3147*Δ*9*-up-F	5'-GATAACATTCGAGTCGACAGAACGA GGAGTTGTTTACC-3'
	*BT3147*Δ*9*-up-R	5'-TTAATCTAGATTTTTTTCTACTAAACCG-3'
	*BT3147*Δ*9*-down-F	5'-CGGTTTAGTAGAAAAAAATCTAGATTAATGA TTTTCGTCTTCCACAAAACGATTG-3'
	*BT3147*Δ*9*-down-R	5'-CTTATCGATACCCTACGGCACAGTTGA GAGATTGGAG-3'
Δ*BT3148*	*BT3148*-up-F	5'- GAAAGAAGATAACATTCGAGGGAAAACGA TGCCTTGGTG -3'
	BT3148-up-R	5'- ATATTTACTTGTTACCGTATTCATCGTCTTTGGT TCTAC - 3'
	BT3148-down-F	5'- AGACGATGAATACGGTAACAAGTAAATATACA ATTAGAA -3'
	BT3148-down-R	5'- ACCGCGGTGGCGGCCGCTTAAACCGTCATGACC ACTTTGA -3'
Δ*BT3148-5*	*BT3148*-up-F	5'- GAAAGAAGATAACATTCGAGGGAAAACGA TGCCTTGGTG -3'
	BT3148-up-R	5'-GTTTTGTGGAAGACGCGTATTCATCGTCTTTGG TTCTAC-'3
	BT3145-down-F	5'-AGACGATGAATACGCGTCTTCCACAAAACGATTG-3'
	BT3145-down-R	5'-ACCGCGGTGGCGGCCGCTGAAACGCAGAAGAGG CTTT-3'
Δ*BT3148-7*	*BT3148*-up-F	5'- GAAAGAAGATAACATTCGAGGGAAAACGA TGCCTTGGTG -3'
	BT3148-up-R	5'-GTTTTGTGGAAGACGCGTATTCATCGTCTTTGG TTCTAC-'3
	BT3147-down-F	5'-AGACGATGAATACGTGACACATTCAATAATTTT AAAC-3'
	BT3147-down-R	5'-ACCGCGGTGGCGGCCGCTTTCGGGCATTGA GGTCATTTA-3'

881

Insertion of *BT1311*	*BT1311* promoter-F	5'-GGGTCTAGATAGTGCCATATGTTAAAAACA

promoter in pNBU2-*bla-erm*		GATTTGGAGTGC-3’
	BT1311 promoter-R	5’-CCCGCGGCCGCTGATCTGGAAGAAGCA ATGAAAGC-3’
Cloning *BT3148-7* in pNBU1311	*BT3148*-F	5’-CCAAATCTGTTTTTAACATATGCTGGTCAT GTTCGTGTGG-3’
	BT3147-R	5’-GTTCTAGATAGTGCTTATTTTGTTATAT CAAAAGC-3’
Cloning of *BT3146-5* in pNBU1311	*BT3146*-F	5’-CCCCATATGAATGATTTCAAGAATCAATGG-3’
	BT3146-R	5’-CCGTCTAGATCAGCCTTTCTTGTTCCACG-3’
Cloning *BT3148-7*Δ*9* in pNBU1311	*BT3148-7*Δ*9*-F	5’- GTTTTTAACATATGGCACTATATGCTGGTCATG TTCGTGTG -3’
	*BT3148-7*Δ*9*-R	5’-AGCCCGGGGGATCCACTAGTTTTAATCTAG ATTTTTTTCTACTAAACCGTCA-3’
Cloning tetQ into pExchange	*tetQ*-F	5’-GGCCATATGAATATTATAAATTTAGGAAT TCTTGCTCAC-3’
	tetQ-R	5’-CCCTCTAGATCGTCTATTTTTTTATTGCCA AGTTCTAATGC-3’
Deletion of *BT3147* upstream of Tn	*BT3148*-up-F	5’-GCGGTCGACAGCAGACCTCTGCTGATAGC-3’
	BT3148-up-R	5’-ACATATCTTCAGATAGATGTATC-3’
	*BT3147**-down-F	5’-GATACATCTATCTGAAGATATGTTTCTACC GGCACTTCTGC-3’
	*BT3147**-down-R	5’-GCGTCTAGACTCTTTGTTAACCC-3’
Localization of Tn	ARB-bt1	5’-GGCCACGCGTCGACTAGTAC NNNNNNNNNGATAT-3’
	ARB-bt-bis	5’-GGCCACGCGTCGACTAGTAC-3’
	pSCIRerm R	5’-GATTTGAACGTTGCGAAGC-3’
	pSCIRerm R-bis	5’-TTTTTGCGTTTCTACCTGC-3’
	pSCIRerm L	5’-CGTATCGGTCTGTATATCAGC-3’
	pSCIRerm L-bis	5’-CTCATCTTTCTGAGTCCACC-3’
DNA contamination check by RT-qPCR	*DNApol3*-F	5’-TGTCGCCCGTCTGGTAGATA-3’
	DNApol3-R	5’-CCGCCTCCTTATCCTCACAC-3’

885 **Table S3. List of strains used in this study**

Strains and plasmids	Relevant characteristics	References[a]
Escherichia coli		
MG1655	K-12 wild-type strain	(2)
S17-1 λ*pir*	(F^-) RP4-2-Tc::Mu aphA::Tn7 recA λpir lysogen. Sm^R, Tp^R	
S17-1 λ*pir_pSAM-bt*	S17-1 λpir derivative carrying pSAM-bt	This study
S17-1 λpir_pExchange-*tdk*	S17-1 λpir derivative carrying pExchange-*tdk*	This study
S17-1 λpir_pNBU2-*bla-erm*	S17-1 λpir carrying pNBU2-*bla-erm*	This study
S17-1 λpir_pExchange-*BT3147*	S17-1 λpir carrying pExchange-*BT3147*	This study
S17-1 λpir_pExchange-*BT3146-5*	S17-1 λpir carrying pExchange-*BT3146-3145*	This study
S17-1 λpir_pExchange-*BT3147Δ9*	S17-1 λpir carrying pExchange-*BT3147Δ9*	This study
S17-1 λpir_pExchange-*BT3148*	S17-1 λpir carrying pExchange-*BT3148*	This study
S17-1 λpir_pExchange-*BT3148-5*	S17-1 λpir carrying pExchange-*BT3148-3145*	This study
S17-1 λpir_pExchange-*BT3148-7*	S17-1 λpir carrying pExchange-*BT3148-3147*	This study
S17-1 λpir_pNBU1311	S17-1 λpir carrying pNBU1311	This study
S17-1 λpir_pNBU1311-*BT3146-5*	S17-1 λpir carrying pNBU1311-*BT3146-3145*	This study
S17-1 λpir_pNBU1311-*BT3148-7*	S17-1 λpir carrying pNBU1311-*BT3148-3147*	This study
S17-1 λpir_pNBU1311-*BT3148-7Δ9*	S17-1 λpir carrying pNBU1311- *BT3148-3147Δ9*	This study
S17-1 λpir_pExchange-*tetQ-BT3147**	S17-1 λpir carrying pExchange-*tetQ-BT3147**	This study
S17-1 λpir_pExchange-*tetQ*	S17-1 λpir carrying pExchange-*tetQ*	This study
Bacteroides thetaiotaomicron		
VPI 5482	Healthy adult human feces	(1)
VPI 5482_*Δtdk*	Deletion of thymidine kinase in the wild type strain ATCC29148	**(3)**
VPI 5482_ *ΔBT3147*	Deletion of *BT3147*	This study
VPI 5482_ *ΔBT3146-5*	Deletion of *BT3146-3145*	This study
VPI 5482 *ΔBT3148-5*	Deletion of *BT3148-3145*	This study
VPI 5482 *ΔBT3148-7*	Deletion of *BT3148-3147*	This study
VPI 5482 *BT3147Δ9*	Deletion of *BT3146-3145* and the last 9 C-terminal amino acids of *BT3147*	This study
VPI 5482 *ΔBT3148 BT3147Δ9*	Deletion of *BT3148* in VPI 5482_ *BT3147Δ9* strain	This study

VPI 5482_p.*BT3146-5*	Chromosomal-based expression of *BT3146-5* from pNBU1311	This study
VPI 5482_p.*BT3148-7*	Chromosomal-based expression of *BT3148-7* from pNBU1311	This study
VPI 5482_p.*BT3148-7 Δ9*	Chromosomal-based expression of BT3148 and the 9 amino acid truncated version of *BT3147* from pNBU1311	This study
VPI 5482_ pNBU2-*bla-erm*	Erythromycin resistant strain	This study
1H2 *ΔBT3147**	1H2 mutant with deletion of *BT3147* portion upstream of the Tn-insertion	This study

Plasmids

pSAM-bt	Random transposon mutagenesis	(Goodman *et al.*, 2009)
pExchange-*tdk*	Site-directed unmarked gene deletion	(Martens *et al.*, 2008)
pNBU2-*bla-erm*	Chromosomal-based gene expression	(Martens *et al.*, 2008)
pNBU1311	Derivative of pNBU2-bla-erm with cloned constitutive promoter of *BT1311* for gene expression	This study
pExchange-*BT3147*	pExchange derivative for unmarked deletion of *BT3147*	This study
pExchange-*BT3146-5*	pExchange derivative for unmarked deletion of *BT3146* and *BT3145*	This study
pExchange-*BT3147Δ9*	pExchange derivative for unmarked deletion of *BT3146-5* and last 9 amino acids of BT3147 C-terminus	This study
pExchange-*BT3148*	pExchange derivative for unmarked deletion of *BT3148*	This study
pExchange-*BT3148-5*	pExchange derivative for unmarked deletion of *BT3148* to *BT3145*	This study
pExchange-*BT3148-7*	pExchange derivative for unmarked deletion of *BT3148* and *BT3147*	This study
pNBU1311-*BT3146-5*	pNBU1311 derivative for expression of *BT3146-5*	This study
pNBU1311-*BT3148-7*	pNBU1311 derivative for expression of *BT3148-7*	This study
pNBU1311-*BT3148-7* $^{\Delta 9}$	pNBU1311 derivative for expression of *BT3148-7* $^{\Delta 9}$	This study
pExchange-*tetQ*	pExchange derivative with erm resistance exchanged for tetracycline	This study
pExchange-*tetQ-BT3147**	pExchange-tetQ derivative for deletion of *BT3147* portion laying upstream of the Tn insertion	This study

[a] Bacterial strains from our laboratory collection unless otherwise specified.
CRBIP**:** *Institut Pasteur, Centre de Resources Biologiques de l'Institut Pasteur.*

1. Xu J, Bjursell MK, Himrod J, Deng S, Carmichael LK, Chiang HC, Hooper LV, Gordon JI. 2003. A genomic view of the human-Bacteroides thetaiotaomicron symbiosis. Science (New York, NY) 299:2074-2076.
2. Guyer MS, Reed RR, Steitz JA, Low KB. 1981. Identification of a sex-factor-affinity site in E. coli as gamma delta. Cold Spring Harb Symp Quant Biol 45 Pt 1:135-40.
3. Koropatkin NM, Martens EC, Gordon JI, Smith TJ. 2008. Starch catabolism by a prominent human gut symbiont is directed by the recognition of amylose helices. Structure (London, England : 1993) 16:1105-1115.

900